

RESEARCH ARTICLE

B7-DC (PD-L2) costimulation of CD4⁺ T-helper 1 response via RGMB

Xinxin Nie¹, Wenni Chen¹, Ying Zhu¹, Baozhu Huang¹, Weiwei Yu¹, Zhanshuai Wu¹, Sizheng Guo¹, Yiping Zhu¹, Liqun Luo¹, Shengdian Wang² and Lieping Chen^{1,3}

The role of B7-DC in T-cell responses remains controversial because both coinhibitory and costimulatory functions have been reported in various experimental systems *in vitro* and *in vivo*. In addition to interacting with the coinhibitory receptor PD-1, B7-DC has also been shown to bind repulsive guidance molecule b (RGMB). The functional consequences of the B7-DC/RGMB interaction, however, remain unclear. More than a decade ago, we reported that replacement of a murine B7-DC mutant lysine with serine (K113S) at positive 113 resulted in a loss of binding capacity to PD-1. Nevertheless, K113S remained costimulatory for T cells *in vitro*, implicating a dual functionality for B7-DC in T-cell responses. Here we show that recombinant K113S protein interacts with RGMB with a similar affinity to wild-type B7-DC. More importantly, K113S costimulates CD4⁺ T-cell responses via RGMB and promotes Th1 polarization. RGMB is expressed on the surface of naive mouse T cells, macrophages, neutrophils and dendritic cells. Finally, K113S/RGMB costimulation suppresses Th2-mediated asthma and ameliorates small airway inflammation and lung pathology in an experimental mouse model. Our findings indicate that RGMB is a costimulatory receptor for B7-DC. These findings from the K113S variant provide not only a possible explanation for the B7-DC-triggered contradictory effects on T-cell responses, but also a novel approach to investigate the B7-DC/PD-1/RGMB axis. Recombinant K113S or its derivatives could potentially be developed as an agonist for RGMB to costimulate the Th1 response without triggering PD-1-mediated T-cell inhibition.

Cellular & Molecular Immunology advance online publication, 8 May 2017; doi:10.1038/cmi.2017.17

Keywords: asthma; B7-DC; K113S; RGMB; Th1/Th2

INTRODUCTION

B7-DC (also called PD-L2, CD273) has been reported as a ligand for programmed death one (PD-1),^{1–3} but its function in the regulation of T-cell responses remains elusive. While several studies support a role for B7-DC in the suppression of T-cell responses via PD-1 engagement on T cells,^{1,4–6} others have shown that B7-DC may costimulate T-cell responses and enhance the immune response.^{3,7–9} Using site-directed mutagenesis, our early work in 2003 showed that a B7-DC variant (K113S, replacing lysine at positive 113 with serine) lost its binding to PD-1 but retained its function in the stimulation of T-cell responses. Based on these findings, we proposed the existence of a new costimulatory receptor for B7-DC.⁸

Recently, B7-DC was found to bind repulsive guidance molecule family member b (RGMB, also called DRAGON).¹⁰ RGMB, a Glycosylphosphatidylinositol-linked membrane-associated protein, contains an N-terminal 50 amino-acid

signal peptide, C-terminal 35 amino-acid Glycosylphosphatidylinositol attachment signal, RGM N-terminus domain, RGM C-terminus domain and a von Willebrand factor type-D domain in the middle of the molecule.^{11,12} RGMB mRNA is widespread in the spinal cord, brain (midbrain, hindbrain and forebrain), liver, kidney, optic nerve and reproductive tract.^{12–14} Studies have shown that RGMB is a coreceptor of BMP2/4 (bone morphogenetic protein 2 and 4, BMP2/4) to enhance Smad phosphorylation responses.^{15,16} RGMB mRNA is also found in epithelial cells,¹⁷ macrophages^{10,16} and dendritic cells.¹⁰ Normal lung interstitial macrophages and alveolar epithelial cells express high levels of RGMB mRNA.^{10,16} In a recent study, blockade of the RGMB/PD-L2 interaction using a monoclonal antibody (mAb) impaired the development of respiratory tolerance.¹⁰ The role of RGMB during the T-cell response to antigen, however, remains unknown.

¹Laboratory of Immunotherapy, Sun Yat-sen University, Guangzhou, Guangdong, China; ²Institute of Biophysics, Chinese Academy of Sciences, Beijing, China and ³Department of Immunobiology, Yale University, New Haven, CT, USA

Correspondence: Dr L Chen, MD, PhD, Department of Immunobiology, Yale University, 300 George Street, New Haven, CT, USA.

E-mail: lieping.chen@yale.edu

Received: 8 February 2017; Accepted: 8 February 2017

Asthma is a chronic small airway disorder characterized by airway obstruction, wheezing airway hyper-responsiveness and recurrent inflammation.¹⁸ Most of this disease arises from exposure to allergens such as pollen, house dust mites, animal dander fungi, molds, air irritants and infections.^{18–20} Different types of immune cells participate in the pathogenesis of asthma, including eosinophils, macrophages, T cells, neutrophils and mast cells.^{18,21} The CD4⁺ T-helper 2 subset (Th2) is an important element in asthma progression. When an allergen stimulates the immune system through the airway of the lung, Th2 cells produce high levels of IL-5, IL-13 and IL-4, which subsequently promote allergen-specific IgE and airway smooth muscle mediators from mast cells.^{22–24} IL-5 can promote eosinophil development, activation and recruitment to the airway of the lung.^{25,26} IL-13 is involved in airway remodeling and airway hyper-responsiveness to promote asthma.^{27,28} The T-helper 1 subset, however, often suppresses Th2-mediated responses, and there is ample evidence indicating that the Th1/Th2 balance is critical for the development of asthma.²⁹ Th1 can mediate the suppression of Th2 responses via the production of interferon- γ (IFN- γ) and IL-12.^{30–32}

RGMB knockout (KO) mice die ~2 weeks after birth, largely due to requirements during neural development.^{16,33} This prevents the use of this strain for further dissection of B7-DC/RGMB functions. As an alternative approach, we first identified a B7-DC variant K113S that selectively binds RGMB but not PD-1. With this unique ligand for RGMB, we explored the role of B7-DC/RGMB interactions in T-cell responses.

MATERIALS AND METHODS

Mice

Female BALB/c mice were purchased from and housed in a specific pathogen-free facility in the Experimental Animal Centre of Sun Yat-sen University. All mouse experiments were carried out in accordance with the Sun Yat-sen University Laboratory Animal Centre guidelines and were approved by the Institutional Animal Care and Use Committee.

Cell lines

A Chinese hamster ovary (CHO) line expressing murine PD-1 was cultured in Ham's F12 medium (Gibco, Gaithersburg, MD, USA) with 1% FBS. The 293T cell line (ATCC, Manassas, VA, USA) was cultured in DMEM (Cellgro, Manassas, VA, USA) with 10% FBS and was transfected with Lipofectamine 3000 transfection reagent and mouse RGMB cDNA in a pEGFP-N3 expression vector. The cell surface expression of RGMB was verified by staining with RGMB antibody (R&D Systems, Minneapolis, MN, USA) and eGFP fluorescence.

Recombinant fusion proteins, antibodies and cytokines

Plasmids encoding the fusion protein of mouse B7-DC-human IgG1Fc (B7-DC-hIg) and its variants have been previously described.⁸ Recombinant proteins were produced by 293T cell transfection and purified using a protein, an affinity column (GE, Chicago, IL, USA).³⁴ Anti-hIg was purchased from Jackson ImmunoResearch (West Grove, PA, USA) and His-

tagged recombinant mouse RGMB and anti-murine RGMB-biotin were purchased from R&D Systems. Streptavidin-PE was purchased from BioLegend (San Diego, CA, USA). Anti-CD3e-PE, anti-CD4-PE, anti-CD8-PE, anti-CD11c-PE, anti-Gr1-PE, anti-B220-PE, anti-CD49b-PE, anti-F4/80-PE, anti-mB7-DC-APC, anti-IL-2-FITC, anti-IFN- γ -PE and anti-IL-4-APC mAb and mouse IL-4, IL-5, IL-13 ELISA kits were purchased from eBioscience (San Diego, CA, USA). Fisher HealthCare PROTOCOL Hema 3 Fixative and Solutions, Inject Alum and carboxyfluorescein succinimidyl ester (CFSE) staining dye were purchased from Thermo Scientific (Waltham, MA, USA). Albumin from chicken egg grade V ovalbumin (OVA) and methacholine were purchased from Sigma-Aldrich (St Louis, MO, USA). Anti-IgE-biotin, Cytofix-CytoPerm with the Golgi-plug kit and anti-CD4-BV421 were purchased from BD (Franklin Lakes, NJ, USA).

Surface plasmon resonance analysis

The affinity of murine RGMB with B7-DC and its variants were analyzed on a Biacore T100 instrument as previously described.⁸ In brief, his-tagged RGMB was immobilized on a CM5 sensor chip (GE Healthcare, Chicago, IL, USA) at 2000 RUs, and the control flow cell was similarly prepared. Purified Flag-hIg, mB7-DC-hIg and variant fusion proteins were diluted in HEPES buffer at the indicated concentrations (mB7-DC-hIg and K113S-hIg from 3.9 to 500 nM, R56S-hIg and E71S-hIg from 109.4 nM to 7 μ M, I105A-hIg, D111S-hIg, R101S-hIg and Flag-hIg at 10 μ M). The proteins were injected at a flow rate of 20 μ l/min for 3 min, and the buffer was passed over the surface for 5 min for dissociation. The data were analyzed using Biacore T100 software.

Experimental asthma mouse model

The OVA-induced asthma mouse model has been previously described.³¹ Briefly, 6–8-week-old BALB/c mice were immunized by intraperitoneally injection of 10 μ g OVA protein (Sigma-Aldrich) mixed with 4 mg aluminum hydroxide gel (Inject Alum, Thermo) on day 0 and day 5. Mice were nasally challenged with 1% OVA in PBS using a nebulizer (Yuwell 402AI, Jiangsu, China) for 30 min on days 11–13. Mice were anesthetized on day 14. Blood was collected from the inferior vena cava, and sera were prepared for OVA-specific IgE detection. Lungs were lavaged with 0.5 ml of warm PBS via a tracheal cannula three times with a total 1 ml of PBS. The bronchoalveolar lavage fluids (BALFs) were centrifuged, and the supernatants were collected for cytokine assays (below). A Coulter counter (Beckman Coulter, San Diego, CA, USA) was used to count the total number of cells. The lungs were also fixed with 10% formalin, and the tissue sections were stained by H/E for histological evaluation. For hydrodynamic injection of plasmids *in vivo*, control Flag-hIg or K113S-hIg plasmid at 20 μ g in a 2-ml volume of PBS were injected within 5–10 s via the tail vein, as previously described.³⁵ Human IgG protein levels in sera and BALF upon hydrodynamic injections were tested by specific sandwich ELISA at the indicated time points (Figures 4b and c).

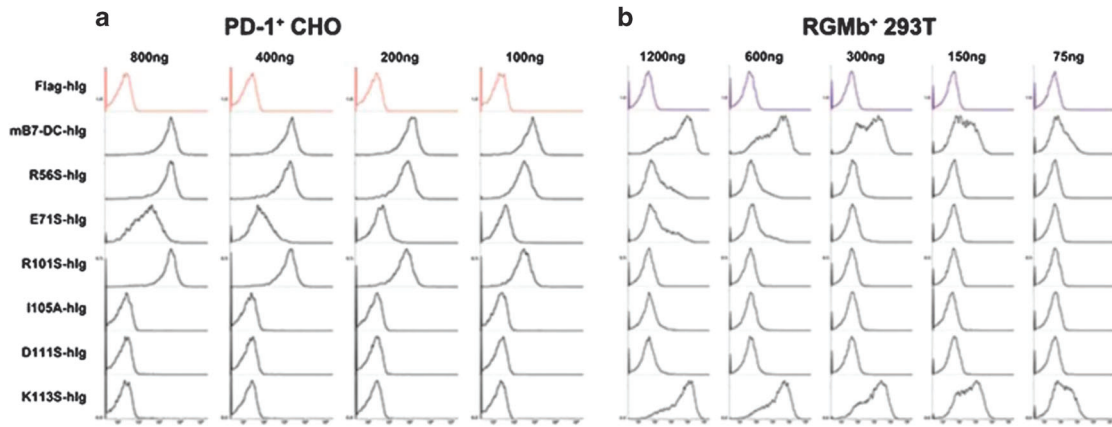


Figure 1 Binding of B7-DC variants to PD-1 or RGMb. (a) CHO cell lines were transfected to overexpress mouse PD-1 (PD-1⁺ CHO) and stained with the indicated concentrations of control Ig (Flag-hlg), B7-DC-hlg or its variants and subsequently analyzed by flow cytometry. (b) 293 cell lines were transfected to overexpress mouse RGMb (RGMb⁺ 293T) and stained with the indicated concentrations of control Ig (Flag-hlg), B7-DC-hlg or its variants and subsequently analyzed by flow cytometry. The second antibody used for staining was mouse anti-human IgG Fc-Alexa Fluor 647. All data are representatives of three or more independent experiments. CHO, Chinese hamster ovary; RGMb, repulsive guidance molecule b.

Table 1 Affinity measurement of B7-DC variants

	<i>K_a</i> (1/Ms)	<i>K_d</i> (1/s)	<i>K_D</i> (M)
B7-DC	2.06E+05	0.03744	1.82E-07
K113S	1.94E+05	0.02473	1.28E-07
R56S	8.78E+05	0.2718	3.10E-06
E71S	1.32E+05	0.3744	2.83E-06

The affinity (KD) was calculated based on Biacore T100 software from 'ka' (association) and 'kd' (dissociation).

Airway hyperresponsiveness assays

Airway hyperresponsiveness to methacholine was evaluated 24 h after the last 1% OVA challenge by both invasive and non-invasive assays.³⁶ The invasive assay was determined using the FinePointe Resistance and Compliance System (Buxco Electronics, NY, USA). Briefly, the mice were anesthetized, and a tracheotomy was performed. PBS, followed by methacholine (12.5, 25 mg/ml), was nebulized and flowed into the trachea of the mice for 30 s. The respiratory flow and lung pressure of the mice were directly measured. Airway resistance (R_L) was defined as the pressure driving respiration divided by the flow, which was computed using Buxco FinePointe Software. The non-invasive assay was determined using the FinePointe Whole Body Plethysmography System (Buxco Electronics, NY, USA),³⁷ which relies on four designed chambers to connect a sensitive pressure transducer to measure pressure changes and flow inside the chamber and transmit information to the Buxco FinePointe Software. The software calculates several flow-derived parameters, including respiratory rate, lung volume, peak flow and time intervals. It reported data as 'enhanced pause' (Penh).³⁷ $Penh = (PEP/PIP) \times ((Te - Tr)/Tr)$. Te , expiratory time (s); Tr , relaxation time (s); PEP, peak expiratory pressure (ml/s); PIP, peak inspiratory pressure (ml/s).³⁷

Mice were individually placed into each chamber and allowed to acclimate for several minutes to record the baseline periods of the chamber. After the baseline measurements, increasing concentrations of methacholine in PBS (0, 3.125, 6.25, 12.5, 25, 50 mg/ml) were nebulized for 1 min in the main chamber through the inlet. The airway responses were then recorded for 5 min. The Penh was computed for each group for the increasing concentrations of methacholine.

Th1 polarization assay *in vitro*

For Th1 generation, CD4⁺ T cells were labeled with CFSE (Thermo Fisher Scientific, MA, USA) at 2 μ M and stimulated with anti-CD3 antibody (clone 145-2C11) at 2.5 μ g/ml and the indicated fusion protein coated on the plate at 5 μ g/ml in the presence of 10 μ g/ml anti-IL-4 and 10 ng/ml IL-12 for 3 days. In the last 6 h, 10 ng/ml phorbol 12-myristate 13-acetate (PMA), 1 μ g/ml ionomycin and 10 μ g/ml brefeldin A were added to the culture, and the cells were stained with anti-CD4 mAb. Upon fixation and permeabilization using the Cytofix/Cytoperm Kit (BD Bioscience, Franklin Lakes, NJ, USA), the cells were stained with mAb against IFN- γ and subjected to flow cytometry analysis. Similar methods were also used to detect IFN- γ , IL-2 and IL-4-positive cells in BALFs. Cytokines in BALF were also measured using an ELISA kit (eBioscience) according to the protocol.

Statistical analysis

Each experiment presented in this report was repeated at least three times; the numbers of animals are stated in the figure legends. The data are presented as the mean \pm s.e.m., followed by the significant difference determined using a two-tailed Student's *t*-test or analysis of variance (ANOVA). * $P < 0.05$, ** $P < 0.01$ and *** $P < 0.001$.

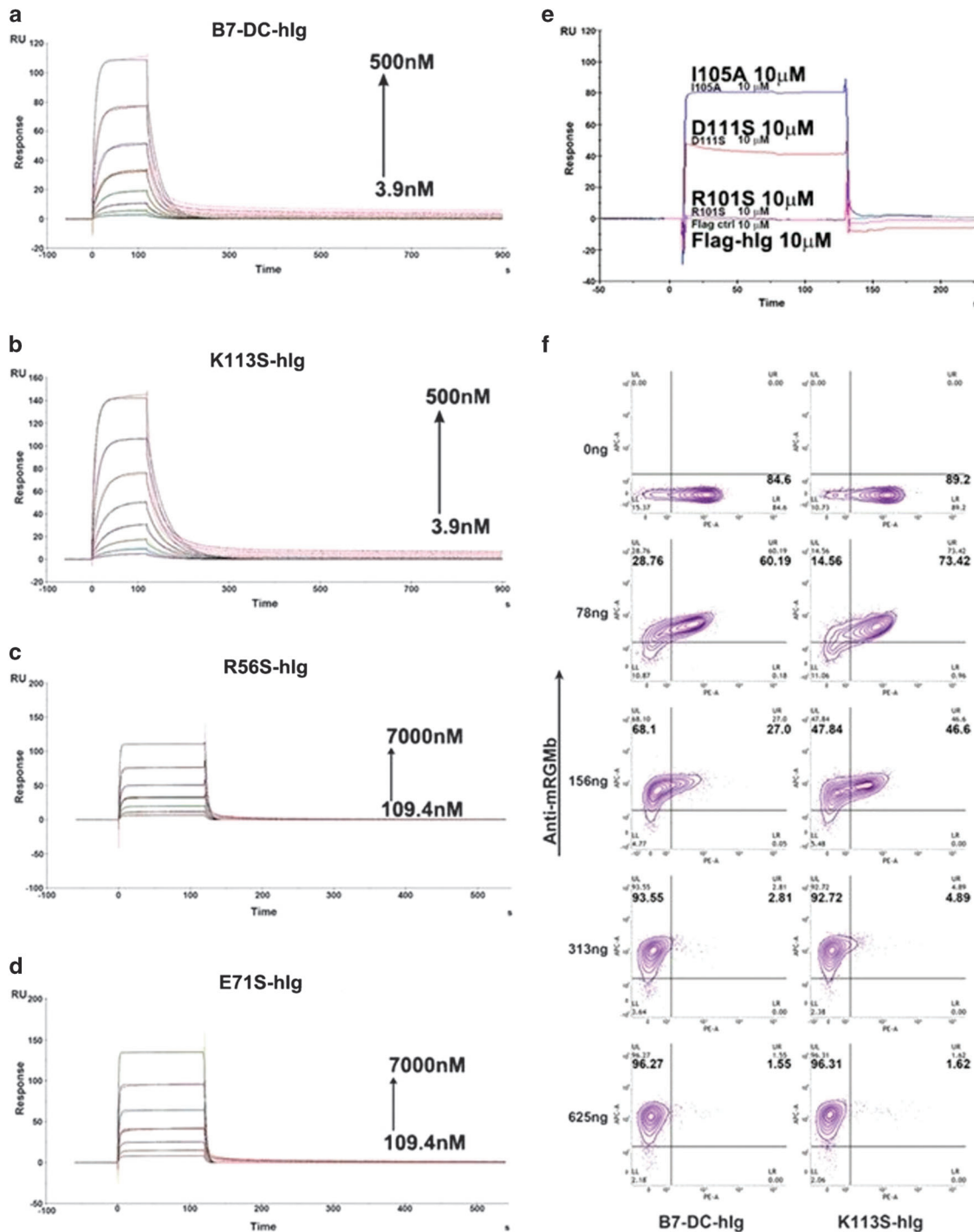


Figure 2 Binding affinity of B7-DC and its variants to RGMB. (a,b) Biacore analysis of the SPR of B7-DC-hlg (a) or K113S-hlg (b) interactions with mouse RGMB, which was coated on the CM5 biosensor chip at various concentrations (3.906–500 nM). (c, d) Biacore analysis of the SPR of R56S-hlg (c) or E71S-hlg (d) interactions with RGMB, which was coated on the chip at various concentrations (0.1094–7 μ M). (e) Response units of the SPR analysis of RGMB interactions with I105A-hlg, D111S-hlg, R101S-hlg and control Flag-hlg at 10 μ M. (f) The 293T cell lines were transfected to overexpress mouse RGMB and stained at the indicated concentrations of anti-mRGMB-biotin (secondary antibody SA-APC) and 1 μ g B7-DC-hlg or K113S-hlg (secondary antibody goat anti-human Fc-PE) and subsequently analyzed by flow cytometry. All data are representatives of three or more independent experiments. RGMB, repulsive guidance molecule b; SPR, surface plasmon resonance.

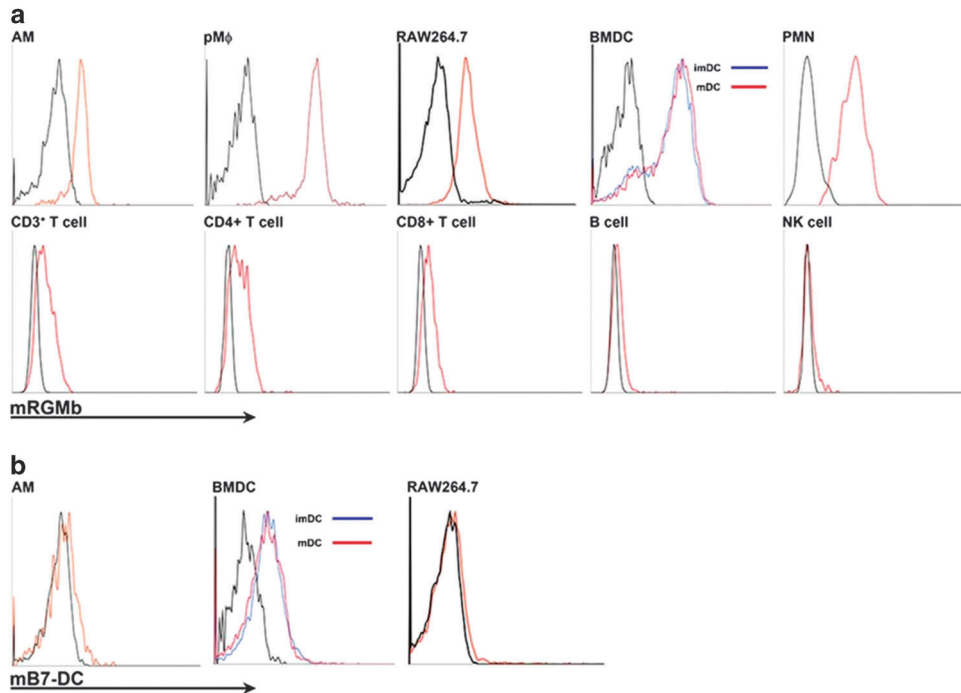


Figure 3 Expression of RGMB and B7-DC on mouse myeloid and lymphoid cells. **(a)** RGMB cell surface expression was examined using a specific polyclonal antibody (R&D Systems) by flow cytometry analysis on AMs, pMφs, BMDCs (immature DCs, blue line; mature DCs, red line), the RAW264.7 macrophage cell line and freshly isolated spleen PMNs, T, B and NK cells. **(b)** B7-DC cell surface expression was tested by flow cytometry on AMs, pMφs, BMDCs (both immature and mature DCs indicated by the blue and red line, respectively) and the RAW264.7 macrophage cell line. All data are representatives of three or more experiments. AMs, alveolar macrophages; BMDCs, bone marrow-derived dendritic cells; pMφs, peritoneal macrophages.

RESULTS

Identification of a B7-DC K113S variant that selectively binds RGMB but not PD-1

We previously demonstrated the generation of several B7-DC variants with mutations in the binding domain of B7-DC and PD-1. A variant, K113S, in which the lysine at amino-acid position 113 was replaced with a serine, completely lost its ability to bind to PD-1. Interestingly, K113S remained costimulatory for lymphocytes *in vitro*.⁸ This finding suggests that B7-DC may function via a receptor other than PD-1 for its costimulatory function. To determine whether K113S interacts with RGMB, we prepared recombinant fusion proteins encoding a set of variants (R56S-hIg, E71S-hIg, R101S-hIg, I105A-hIg, D111S-hIg and K113S-hIg) and tested their binding capacity to RGMB. Using flow cytometry, we showed that I105A, D111S and K113S variants did not bind PD-1⁺ CHO cells at all tested concentrations, while R56S, E71S and R101S variants, and wild-type B7-DC significantly bound to PD-1 (Figure 1a), which was similar to our previous finding.⁸ Interestingly, K113S-hIg bound to RGMB⁺ 293T cells similar to wild-type B7-DC-hIg (Figure 1b), while R101S, I105A and D111S completely lost their ability to bind to RGMB. R56S and E71S appeared to exhibit weak binding to RGMB at high protein concentrations. The above data confirm that B7-DC interacts with both RGMB and PD-1, while K113S was newly found to selectively bind to RGMB but not to PD-1.

K113S binds to RGMB with a similar affinity to wild-type B7-DC

We determined the binding affinity for K113S by performing a surface plasmon resonance (SPR) analysis using the Biacore instrument; the affinity was calculated using Biacore T100 software. K113S bound RGMB with an affinity similar to B7-DC at nM levels (B7-DC KD=1.82E-07 M, K113S KD=1.28E-07; Table 1 and Figures 2a and b), while R56S, E71S, I105A and D111S bound RGMB at μM levels (Figures 2c–e) and R101S at a similar level as the Flag-hIg control (Figure 2e).

To further validate the interaction between K113S and RGMB, we tested the capacity of the RGMB antibody to compete for the binding of K113S and B7-DC to RGMB. The RGMB antibody (at various concentrations up to 625 ng/ml) was added to the culture to compete with B7-DC or the K113S fusion protein (1 μg/ml) for binding to RGMB⁺ 293T cells using flow cytometry. Consistent with the Biacore analysis, the RGMB antibody was slightly less efficient to compete with K113S-hIg than B7-DC-hIg for binding to RGMB⁺ 293T cells in most of the tested concentrations (Figure 2f). Therefore, lysine at amino-acid 113 is crucial for the interaction of B7-DC with PD-1 but not with RGMB, indicating that the K113S variant is a highly selective RGMB ligand that can efficiently avoid PD-1-mediated suppression of T cells.

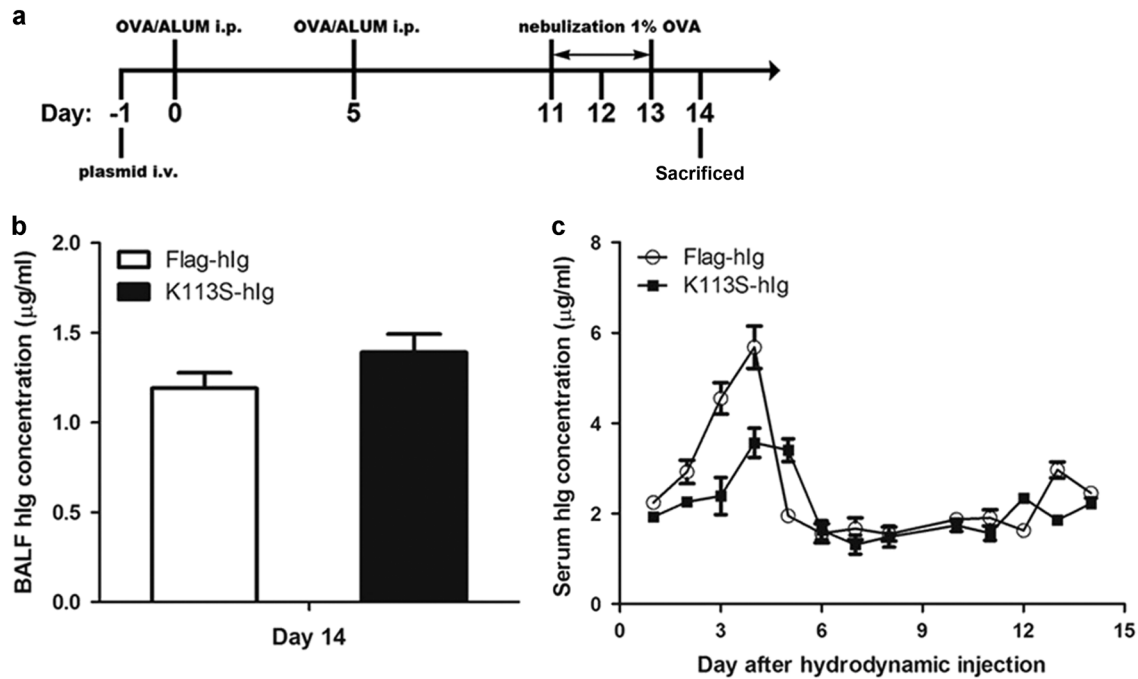


Figure 4 OVA-induced asthma mouse model and fusion protein levels in BALF and serum. (a) Sensitization and challenge protocol for OVA-induced asthma and treatment. BALB/c mice were inoculated i.p. with 10 μg grade V OVA and 1 mg alum gel in PBS on days 0 and 5. The mice were subsequently challenged by inhalation of 1% OVA in PBS for 30 min on days 11–13. One day before the first OVA immunization, plasmids (Flag-hlg and K113S-hlg) were injected i.v. via the tail vein at 20 μg per mouse in 2 ml PBS within 5–10 s. (b) Flag-hlg and K113S-hlg levels in BALF at day 14 after immunization. (c) Flag-hlg and K113S-hlg levels in sera at the indicated days after hydrodynamic injection. The data represent the mean \pm s.e.m., and samples were obtained from five individual mice from each group. The data are representatives of at least three independent experiments. BALF, bronchoalveolar lavage fluids; i.p., intraperitoneally; i.v., intravenously; PBS, phosphate-buffered solution.

Constitutive expression of RGMB on murine lymphocytes and myeloid cells

Using the RGMB antibody, we analyzed RGMB protein expression on various immune cells. RGMB appeared to be constitutively expressed at high levels on myeloid cells, including freshly isolated alveolar macrophages (AMs), peritoneal macrophages (pM ϕ s), bone marrow dendritic cells (BMDCs) and neutrophils (PMNs) and the RAW264.7 macrophage-like cell line, with the highest expression detected on pM ϕ s (Figure 3a). Interestingly, RGMB protein could also be detected at low levels on the surface of resting CD3⁺, CD4⁺ and CD8⁺ T cells and B cells of splenocytes, while NK cells were negative (Figure 3a). The expression of B7-DC, however, was limited to BMDCs, while its expression levels on AMs and RAW264.7 was minimal (Figure 3b) similar to a previous report.³

Engagement of RGMB suppresses lung inflammation and airway hypersensitivity

Taking advantage of RGMB-specific binding by K113S, we examined the function of RGMB in an OVA-induced asthma mouse model in which the mice were first immunized and later challenged with OVA (Figure 4a). In this model, the mice developed Th2-like inflammatory responses with heavy eosinophil infiltration.^{25,28,38} One day before immunization, the mice were injected intravenously with the K113S-hlg plasmid

under high pressure (hydrodynamic injection) to force high levels of plasmid expression (Figures 4b and c), mainly in the liver.³⁵ As expected, the total infiltrating cell numbers in the BALF were dramatically increased upon challenge with OVA. In contrast, mice treated with K113S-hlg exhibited significantly decreased total cell numbers (Figure 5a). The number of eosinophils, the primary cell type observed during OVA-induced asthma, was also significantly suppressed by K113S-hlg (Figures 5a and b). Histological analysis of the lung showed that K113S-hlg-treated mice had significantly less inflammatory infiltration around the small airways compared with those treated with control plasmid (Figure 5c).

Airway hypersensitivity airway hyperresponsiveness was assessed by the resistance of lung (R_L) and Penh, an index of airway hypersensitivity, in this model, as described in the Materials and Methods section. The baseline R_L showed no significant differences among mice treated with the control or K113S plasmids. However, the R_L of 12.5 mg/ml methacholine challenge was decreased in K113S-hlg-treated mice vs Flag-hlg-treated mice (Figure 5d). Furthermore, Penh was significantly reduced in mice treated with K113S-hlg compared with Flag-hlg (Figure 5d). These results indicate that the triggering of RGMB by K113S-hlg suppresses OVA-induced asthmatic inflammation and improves lung function in this experimental asthma model.

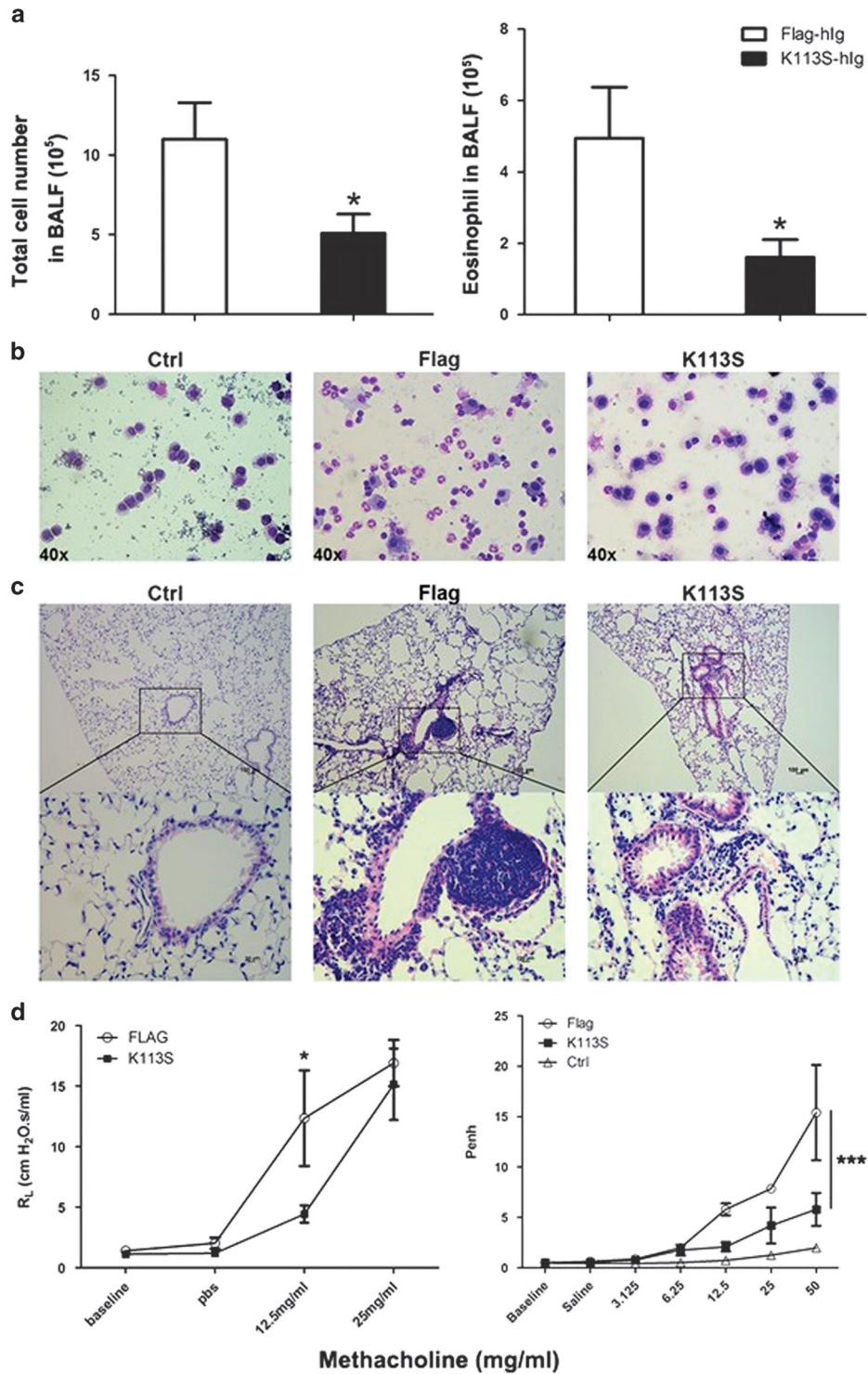


Figure 5 Effect of K113S variants in an OVA-induced mouse model of asthma. (a) The total cell and eosinophil number in BALF from mice after asthma induction with Flag-hlg and K113S-hlg treatment. (b) Cells in BALF from Flag-hlg or K113S-hlg-treated mice were stained with Diff-Quick dye liquor. (c) Lung histology from mice treated with Flag-hlg or K113S-hlg. The mice were killed on day 14, and the lung tissues were processed and stained with H&E to observe the cell infiltration around the small airway. (d) AHR to methacholine challenge. Mice were treated with Flag-hlg and K113S-hlg and were measured for airway resistance and Penh of the lung. The data represent the mean \pm s.e.m. and encompass three independent experiments with five mice in each group. NS, no significant difference; * $P < 0.05$; ** $P < 0.01$; *** $P < 0.001$. BALF, bronchoalveolar lavage fluids; CFSE, carboxyfluorescein succinimidyl ester; H&E, hematoxylin and eosin.

K113S costimulates Th1 responses via RGMB

We hypothesized that K113S-induced suppression of asthma inflammation is caused by costimulation of the Th1 T-cell response, which subsequently suppresses Th2-like

inflammation. To test this hypothesis, we first evaluated the ability of K113S to stimulate the Th1 response during naive CD4⁺ T-cell differentiation into Th1 cells *in vitro*. In this system, purified naive T cells were cultured under Th1

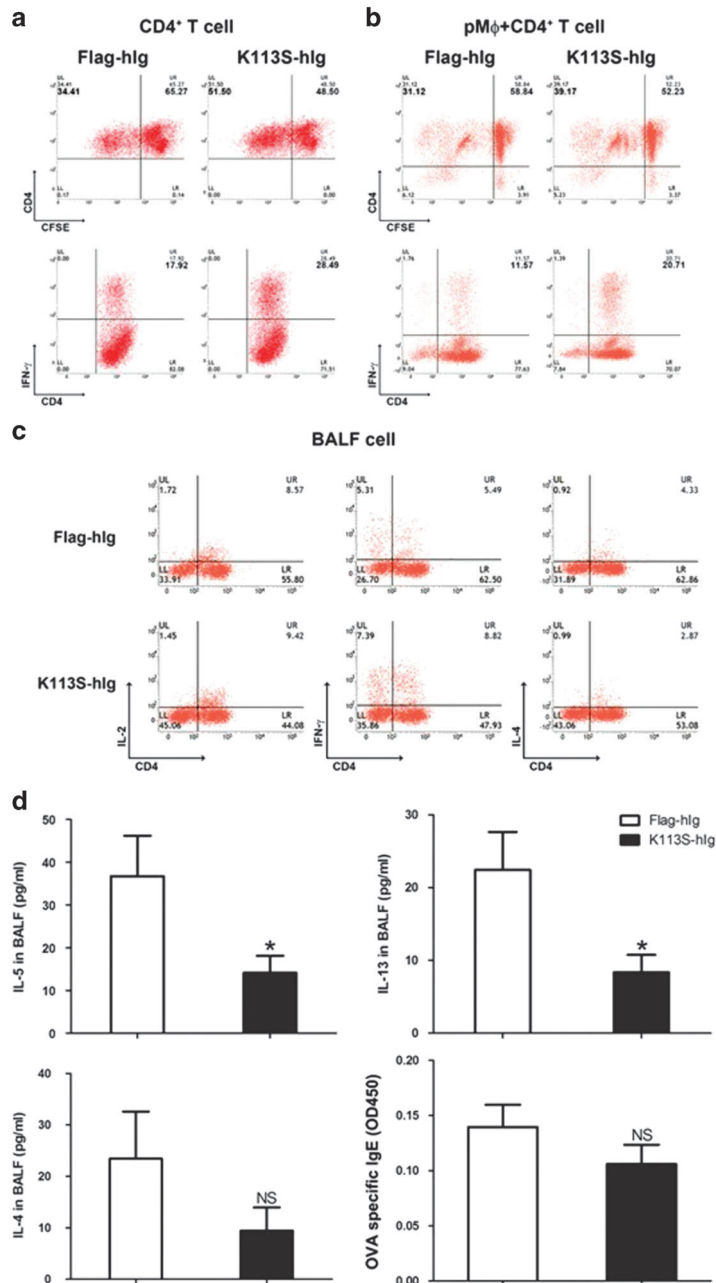


Figure 6 Effect of K113S on CD4⁺ T-cell costimulation and Th1/Th2 cytokine production. (a, b) Purified CD4⁺ T cells from naive BALB/c mice were labeled with CFSE and stimulated under Th1 differentiation conditions (IL-2 10 ng/ml, IL-12 10 ng/ml and anti-IL-4 10 μg/ml) in the absence (a) or presence (b) of pMφs on pre-coated plates with anti-CD3 at 2.5 μg/ml and soluble anti-CD28 at 1 μg/ml for 3 days. CFSE dilution and IFN-γ intracellular staining were evaluated by flow cytometry. (c) Intracellular IL-2, IFN-γ and IL-4 were assayed by flow cytometry using a specific mAb in CD4 cells from the lung following treatment with Flag-hlg or K113S-hlg during OVA-induced asthma. On day 14 after asthma induction, cells from the BALF were stimulated with PMA/ionomycin/brefeldin A for 4–6 h and collected for flow cytometry analysis. (d) Intracellular IL-5, IL-13 and IL-4 were assayed using a specific mAb by ELISA in BALF and OVA-specific IgE in sera following treatment with Flag-hlg or K113S-hlg during OVA-induced asthma. The data are representative of at least three independent experiments consisting of five mice in each group. **P*<0.05. BALF, bronchoalveolar lavage fluids; CFSE, carboxyfluorescein succinimidyl ester; IFN-γ, interferon-γ; NS, no significant difference; PMA, phorbol 12-myristate 13-acetate; pMφs, peritoneal macrophages.

polarization conditions (anti-CD3⁺IL-12/anti-IL-4) for 3 days; Th1 CD4⁺ T cells were identified as IFN- γ -producing cells by intracellular staining. To model the potential involvement of macrophages *in vivo*, pM ϕ s were also added to this culture system. In the presence of K113S-hIg, IFN- γ ⁺ T cells significantly increased in comparison to control Ig (Figures 6a and b). To confirm this finding, intracellular cytokines in T cells from the lungs of mice with OVA-induced asthma were measured by flow cytometry. K113S treatment significantly increased IFN- γ levels in BALF, while the changes in IL-2 and IL-4 were negligible (Figure 6c). In the OVA-induced asthma model, IL-4, IL-5 and IL-13 play an essential role in initiating and maintaining inflammatory responses in airways,^{25,28} while allergen-specific IgE may also play a role in the pathogenesis of asthma.³⁹ Therefore, we measured these cytokines in BALF and OVA-specific IgE in sera. Significantly decreased IL-5 and IL-13 secretion was observed in mice treated with K113S-hIg plasmid. IL-4 and specific IgE production showed a decreased tendency, but this difference was not significant ($P=0.12$ and $P=0.06$, respectively) compared with the control (Figure 6d). The above results indicate that RGMB engagement by K113S selectively costimulates the IFN- γ -producing Th1 response, thereby reducing IL-5 and IL-13 production and suppressing the symptoms of asthma.

DISCUSSION

In this study, we identified K113S, a B7-DC variant with a selective binding capacity for RGMB but not PD-1. We showed that K113S triggered RGMB to costimulate CD4⁺ T-cell growth with a bias toward the Th1 response as evidenced by increased IFN- γ production under Th1 differentiation conditions. Naive T cells constitutively expressed RGMB on their surface. Finally, K113S treatment in an experimental murine asthma model enhanced IFN- γ production in BALF, accompanied by the suppression of IL-5 and IL-13 production. Ultimately, our results support a role for RGMB as a costimulatory molecule leading to CD4⁺ Th1 responses.

Our findings provide an explanation for the contradictory data acquired in the B7-DC studies, in which both positive and negative effects on T cells have been reported.^{1,3,7-9,40} During the priming phase, B7-DC on dendritic cells may costimulate naive CD4⁺ T cells via RGMB, favoring Th1 T-cell proliferation and differentiation. Upon costimulation and activation, T cells are induced to express PD-1, which, upon engagement with B7-DC, transmits a suppressive signal to T cells. In the context of constitutive expression of B7-DC by dendritic cells, the costimulatory function of B7-DC may be quickly attenuated by its PD-1 engagement, which may constitute a safeguard to prevent further expansion and overactivation of T cells. Therefore, depending on the timing and levels of RGMB and PD-1 receptors, B7-DC may display different and sometime opposite effects on T-cell responses. While it has yet to be determined whether human RGMB has similar expression patterns and, more importantly, can also be costimulated upon engagement by B7-DC, our study provides a rationale to explore this possibility.

The mechanism of RGMB-mediated costimulation remains to be fully elucidated, but our findings in the OVA-induced asthma model indicate that K113S could attenuate the asthma response and improve lung function by reducing respiratory inflammation and resistance. Both the total inflammatory cell number and eosinophils in the BALF were alleviated after K113S treatment. Furthermore, pathological inflammation around the small airways in the lung was also abated by this treatment. While it is possible that triggering RGMB directly suppresses the Th2 response, including IL-5 and IL-13 production, eosinophil infiltration and airway remodeling during asthma progression, increased IFN- γ was detected in the BALF. These findings support the costimulation of the Th1 response. The role of the Th1 response in the suppression of Th2-mediated asthma has been well documented.^{29,30} Therefore, costimulation via RGMB promotes Th1 polarization, leading to suppression of the Th2 response. It is worth mentioning that the effect of RGMB is somewhat unique and may not be considered a typical 'Th1-like' response. In our study, although IFN- γ production significantly increased, there was minimal change in the levels of IL-2, another important Th1 cytokine. However, the inhibitory effect of RGMB on the 'Th2-like' response is somewhat partial, as indicated, mainly by the suppression of IL-5 and IL-13. Therefore, the role of RGMB in Th1 polarization may be unique with only a partial effect.

RGMB KO is lethal in mice, and specific agonists for RGMB (either antibodies or small molecules) are not yet available, which limits further exploration of the functions of RGMB. Selective binding of K113S to RGMB, but not PD-1, provides a novel approach for the study of immune regulation mediated by the B7-DC/PD-1/RGMB axis. Recombinant K113S or its derivatives might be developed as an agonist for RGMB to costimulate the Th1 response without triggering PD-1 inhibition of T-cell functions. This approach is also useful for the potential therapeutic manipulation of human diseases including asthma.

CONFLICT OF INTEREST

LC is an advisor/board member for Pfizer, AstraZeneca, NextCure, GenomiCare and Vcanbio and received research support from Boehringer Ingelheim, Pfizer and NextCure. LC is also an uncompensated adjunct faculty member of Sun Yat-sen University. The other authors declare no competing financial interests.

ACKNOWLEDGEMENTS

We thank Jingjing Song for support of the lung function assays and Beth Cadugan for editing the manuscript. This study is partially supported by grants from Guangdong Province Innovative Research Program Project (No. 2011Y035), 863 Project grants to Sun Yat-sen University and the United Technologies Corporation endowed chair from Yale University.

AUTHOR CONTRIBUTIONS

LC and XN developed the concept and designed the experiments. WC, YZ, BH, WY, ZW, SG, YZ, LL and SW performed and/or advised the experiments.

- 1 Latchman Y, Wood CR, Chernova T, Chaudhary D, Borde M, Chernova I *et al*. PD-L2 is a second ligand for PD-1 and inhibits T cell activation. *Nat Immunol* 2001; **2**: 261–268.
- 2 Chen L, Flies DB. Molecular mechanisms of T cell co-stimulation and co-inhibition. *Nat Rev Immunol* 2013; **13**: 227–242.
- 3 Tseng SY, Otsuji M, Gorski K, Huang X, Slansky JE, Pai SI *et al*. B7-DC, a new dendritic cell molecule with potent costimulatory properties for T cells. *J Exp Med* 2001; **193**: 839–846.
- 4 Rodig N, Ryan T, Allen JA, Pang H, Grabie N, Chernova T *et al*. Endothelial expression of PD-L1 and PD-L2 down-regulates CD8(+) T cell activation and cytotoxicity. *Eur J Immunol* 2003; **33**: 3117–3126.
- 5 Ghiotto M, Gauthier L, Serriari N, Pastor S, Truneh A, Nunes JA *et al*. PD-L1 and PD-L2 differ in their molecular mechanisms of interaction with PD-1. *Int Immunol* 2010; **22**: 651–660.
- 6 Ishida M, Iwai Y, Tanaka Y, Okazaki T, Freeman GJ, Minato N *et al*. Differential expression of PD-L1 and PD-L2, ligands for an inhibitory receptor PD-1, in the cells of lymphohematopoietic tissues. *Immunol Lett* 2002; **84**: 57–62.
- 7 Shin T, Yoshimura K, Shin T, Crafton EB, Tsuchiya H, Housseau F *et al*. *In vivo* costimulatory role of B7-DC in tuning T helper cell 1 and cytotoxic T lymphocyte responses. *J Exp Med* 2005; **201**: 1531–1541.
- 8 Wang S, Bajorath J, Flies DB, Dong H, Honjo T, Chen L. Molecular modeling and functional mapping of B7-H1 and B7-DC uncouple costimulatory function from PD-1 interaction. *J Exp Med* 2003; **197**: 1083–1091.
- 9 Shin T, Kennedy G, Gorski K, Tsuchiya H, Koseki H, Azuma M *et al*. Cooperative B7-1/2 (CD80/CD86) and B7-DC costimulation of CD4(+) T cells independent of the PD-1 receptor. *J Exp Med* 2003; **198**: 31–38.
- 10 Xiao YP, Yu SH, Zhu BG, Bedoret D, Bu X, Francisco LM *et al*. RGMB is a novel binding partner for PD-L2 and its engagement with PD-L2 promotes respiratory tolerance. *J Exp Med* 2014; **211**: 943–959.
- 11 Bell CH, Healey E, van Erp S, Bishop B, Tang C, Gilbert RJ *et al*. Structure of the repulsive guidance molecule (RGM)-neogenin signaling hub. *Science* 2013; **341**: 77–80.
- 12 Severny CJ, Shinde U, Rotwein P. Molecular biology, genetics and biochemistry of the repulsive guidance molecule family. *Biochem J* 2009; **422**: 393–403.
- 13 Li J, Ye L, Sanders AJ, Jiang WG. Repulsive guidance molecule B (RGMB) plays negative roles in breast cancer by coordinating BMP signaling. *J Cell Biochem* 2012; **113**: 2523–2531.
- 14 Kanomata K, Kokabu S, Nojima J, Fukuda T, Katagiri T. DRAGON, a GPI-anchored membrane protein, inhibits BMP signaling in C2C12 myoblasts. *Genes Cells* 2009; **14**: 695–702.
- 15 Babitt JL, Huang FW, Wrighting DM, Xia Y, Sidis Y, Samad TA *et al*. Bone morphogenetic protein signaling by hemojuvelin regulates hepcidin expression. *Nat Genet* 2006; **38**: 531–539.
- 16 Xia Y, Cortez-Retamozo V, Niederkofler V, Salie R, Chen S, Samad TA *et al*. Dragon (repulsive guidance molecule b) inhibits IL-6 expression in macrophages. *J Immunol* 2011; **186**: 1369–1376.
- 17 Liu W, Li X, Zhao Y, Meng XM, Wan C, Yang B *et al*. Dragon (repulsive guidance molecule RGMB) inhibits E-cadherin expression and induces apoptosis in renal tubular epithelial cells. *J Biol Chem* 2013; **288**: 31528–31539.
- 18 Busse WW, Lemanske RF Jr. Asthma. *N Engl J Med* 2001; **344**: 350–362.
- 19 Baldacci S, Maio S, Cerrai S, Sarno G, Baiz N, Simoni M *et al*. Allergy and asthma: effects of the exposure to particulate matter and biological allergens. *Respir Med* 2015; **109**: 1089–104.
- 20 Kanchongkittiphon W, Gaffin JM, Phipatanakul W. The indoor environment and inner-city childhood asthma. *Asian Pac J Allergy Immunol* 2014; **32**: 103–110.
- 21 Holgate ST. Innate and adaptive immune responses in asthma. *Nat Med* 2012; **18**: 673–683.
- 22 Mosmann TR, Moore KW. The role of IL-10 in crossregulation of TH1 and TH2 responses. *Immunol Today* 1991; **12**: A49–A53.
- 23 Halwani R, Al-Muhsen S, Hamid Q. Airway remodelling in asthma. *Curr Opin Pharmacol* 2010; **10**: 236–245.
- 24 Steinke JW, Borish L. Th2 cytokines and asthma. Interleukin-4: its role in the pathogenesis of asthma, and targeting it for asthma treatment with interleukin-4 receptor antagonists. *Respir Res* 2001; **2**: 66–70.
- 25 Hamelmann E, Gelfand EW. IL-5-induced airway eosinophilia—the key to asthma? *Immunol Rev* 2001; **179**: 182–191.
- 26 Hilvering B, Xue L, Pavord ID. Evidence for the efficacy and safety of anti-interleukin-5 treatment in the management of refractory eosinophilic asthma. *Thorax* 2015; **9**: 135–145.
- 27 Kasaian MT, Miller DK. IL-13 as a therapeutic target for respiratory disease. *Biochem Pharmacol* 2008; **76**: 147–155.
- 28 Wills-Karp M. Interleukin-13 in asthma pathogenesis. *Immunol Rev* 2004; **202**: 175–190.
- 29 Neurath MF, Finotto S, Glimcher LH. The role of Th1/Th2 polarization in mucosal immunity. *Nat Med* 2002; **8**: 567–573.
- 30 Tang F, Wang F, An, Wang L. X. Upregulation of Tim-3 on CD4(+) T cells is associated with Th1/Th2 imbalance in patients with allergic asthma. *Int J Clin Exp Med* 2015; **8**: 3809–3816.
- 31 Luo L, Zhu G, Xu H, Yao S, Zhou G, Zhu Y *et al*. B7-H3 promotes pathogenesis of autoimmune disease and inflammation by regulating the activity of different T cell subsets. *PLoS One* 2015; **10**: e0130126.
- 32 Gavett SH, O’Hearn DJ, Li X, Huang SK, Finkelman FD, Wills-Karp M. Interleukin 12 inhibits antigen-induced airway hyperresponsiveness, inflammation, and Th2 cytokine expression in mice. *J Exp Med* 1995; **182**: 1527–1536.
- 33 Samad TA, Srinivasan A, Karchewski LA, Jeong SJ, Campagna JA, Ji RR *et al*. DRAGON: a member of the repulsive guidance molecule-related family of neuronal- and muscle-expressed membrane proteins is regulated by DRG11 and has neuronal adhesive properties. *J Neurosci* 2004; **24**: 2027–2036.
- 34 Wang SD, Zhu GF, Tamada K, Chen LP, Bajorath J. Ligand binding sites of inducible costimulator and high avidity mutants with improved function. *J Exp Med* 2002; **195**: 1033–1041.
- 35 Azuma T, Zhu G, Xu H, Rietz AC, Drake CG, Matteson EL *et al*. Potential role of decoy B7-H4 in the pathogenesis of rheumatoid arthritis: a mouse model informed by clinical data. *PLoS Med* 2009; **6**: e1000166.
- 36 McGee HS, Yagita H, Shao Z, Agrawal DK. Programmed death-1 antibody blocks therapeutic effects of T-regulatory cells in cockroach antigen-induced allergic asthma. *Am J Respir Cell Mol Biol* 2010; **43**: 432–442.
- 37 Hamelmann E, Schwarze J, Takeda K, Oshiba A, Larsen GL, Irvin CG *et al*. Noninvasive measurement of airway responsiveness in allergic mice using barometric plethysmography. *Am J Resp Crit Care* 1997; **156**: 766–775.
- 38 Kim HY, DeKruyff RH, Umetsu DT. The many paths to asthma: phenotype shaped by innate and adaptive immunity. *Nat Immunol* 2010; **11**: 577–584.
- 39 Platts-Mills TA. The role of immunoglobulin E in allergy and asthma. *Am J Respir Crit Care Med* 2001; **164**: S1–S5.
- 40 Zhang Y, Chung Y, Bishop C, Daugherty B, Chute H, Holst P *et al*. Regulation of T cell activation and tolerance by PDL2. *Proc Natl Acad Sci USA* 2006; **103**: 11695–11700.